ELSEVIER

Thermochimica Acta 317 (1998) 73–84

thermochimica acta

Results of thermal and hydrothermal treatment of the aluminosilicate gels prepared at different batch concentrations

Ivan Krznarić[a], Tatjana Antonić[a], Boris Subotić[a,*], Vesna Babić-Ivančić[b]

[a] *Ruđer Bošković Institute, Laboratory for the Synthesis of New Materials, PO Box 1016, 10001 Zagreb, Croatia*
[b] *Ruđer Bošković Institute, Laboratory for Precipitation Processes, PO Box 1016, 10001 Zagreb, Croatia*

Received 9 February 1998; received in revised form 27 April 1998; accepted 5 May 1998

Abstract

The results obtained during the thermal (thermogravimetry, TG, and differential thermal gravimetry, DTG) and the hydrothermal (heating at 80°C for appropriate time) treatment of the gels prepared at different batch concentrations $[Al_2O_3]_{bN}$ and different batch molar ratios $[SiO_2/Al_2O_3]_{bN}$, are presented. The presence of structurally ordered subunits (quasicrystalline zeolite phase) formed in the gel matrix during its precipitation, causes the appearance of higher-temperature minimum (peak-2) in the DTG curves of the precipitated solids. The intensity of the higher-temperature minimum increases with increasing concentration of structurally ordered subunits (quasicrystalline zeolite phase) in the gel matrix. The increase in concentration of structurally ordered subunits in the solids precipitated at increased batch concentration $[Al_2O_3]_{bN}$ is caused rather by the increase in batch alkalinity than by the increase in concentration of the aluminosilicate part of the system. The influence of alkalinity on the formation of structurally ordered subunits in the gel matrix is explained by the 'olation' condensation mechanism. © 1998 Elsevier Science B.V.

Keywords: Aluminosilicate gels; Chemical composition; Thermal analysis; Hydrothermal treatment; Phase analysis; Particle-size distribution

1. Introduction

Thermal analysis has frequently been used for the characterization of different kinds of minerals, including zeolites and clays [1–3]. The results of simultaneous thermal analysis can give useful quantitative and/or semi-quantitative information on the process of dehydration and thermal stability of different types of zeolites [4–7]. Studying the cited papers, it may be concluded that the results of thermal analysis are very sensitive to the nature of cations present in the aluminosilicate environment and to the interactions of cations with the zeolite framework. Consequently, the results of thermal analysis can give useful information on the pore structure, catalytic activity, degree of hydration of cations in the structure of zeolites and amorphous aluminosilicates, interactions of hydrated cations with aluminosilicate matrix, etc.

In addition, thermal analysis is a very sensitive method for the detection of very small structurally ordered units having a zeolite structure, distributed through the matrix of aluminosilicate gels [8–10]. For

*Corresponding author. Tel.: +385 1 4680123; fax: +385 1 4680084; e-mail: subotic@rudjer.irb.hr

PII S0040-6031(98)00371-2

instance, the differential thermogravimetry (DTG) curve of the gel prepared by potassium aluminate and potassium silicate have only one minimum below 100°C. This minimum corresponds to the removal of loosely held moisture from within the solid microstructure of the gel. An increase of the fraction f_{Na} of the 'structure-forming' sodium ions in the gels formed from mixed Na, K-silicates and aluminates causes the appearance of an additional minimum in their DTG curves. The position of the additional minimum is the same as the position of the minimum in the DTG curve of the crystalline phase (mixture of zeolites A and X) obtained by the hydrothermal treatment of the gels [9,10]. Based on the earlier electron diffraction [11] and IR spectroscopy [12] studies of aluminosilicate gels, it was concluded that the appearance of the higher-temperature minimum is caused by the formation of ordered structural subunits or even more complex structures inside the gel matrix during its precipitation in the sodium or mixed sodium-lithium environment [9,10]. Pursuing the concept of the formation of structurally ordered subunits inside the amorphous gel [13] and their role in nucleation of zeolites [13–15], the influence of the fine structure of aluminosilicate gels (presence of structurally ordered subunits) on the rate of water desorption from the gels and profile of their DTG curves was indicated by the results of the hydrothermal treatment of the gels in 2 M NaOH solution at 80°C [16]: the specific number of crystals of zeolite A obtained by the hydrothermal treatment of sodium and sodium-lithium gel is considerably larger (5.45×10^{10} crystals/g and 5.57×10^{10} crystals/g, respectively) than the specific number of crystals (3.19×10^{10} crystals/g) obtained by the hydrothermal treatment of potassium gel, i.e. sodium and sodium-lithium gels contain much more particles of ordered structural subunits (potential nuclei) than potassium gel.

Based on the above mentioned findings, the subject of this paper is an analysis of the results obtained during the thermal (differential thermogravimetry) and hydrothermal treatments of the gels prepared at different batch concentrations and different molar ratios SiO_2/Al_2O_3, in order to define the influence of the mentioned factors on the water content, structural properties of the gels and type(s) and particulate properties of the zeolite(s) obtained by the hydrothermal treatment.

2. Experimental

Amorphous aluminosilicate hydrogels having the batch compositions: System (hydrogels) I: $3Na_2O{\cdot}Al_2O_32SiO_2{\cdot}Z_IH_2O$, System (hydrogels) II: $4.15Na_2O{\cdot}Al_2O_3{\cdot}3.47SiO_2{\cdot}Z_{II}H_2O$, System (hydrogels) III: $9.06Na_2O{\cdot}Al_2O_3{\cdot}8.05SiO_2{\cdot}Z_{III}H_2O$, and System (hydrogels) IV: X_{IV} $Na_2O{\cdot}Al_2O_3{\cdot}2SiO_2{\cdot}Z_{IV}H_2O$ were prepared as described earlier [17], by pipetting 50 ml of sodium silicate solution of appropriate concentration with respect to Na_2O and SiO_2 into a plastic beaker containing 50 ml of stirred (by a propeller) sodium aluminate solution of appropriate concentration with respect to Na_2O and Al_2O_3. Sodium aluminate solutions (0.025–0.4 M in Al_2O_3) were prepared by dissolution of anhydrous $NaAlO_2$ (54% Al_2O_3 and 41% Na_2O) in distilled water. Sodium silicate solutions were prepared by dilution of water-glass solution (9.086% Na_2O, 26.832% SiO_2) in sodium hydroxide solutions of appropriate concentrations. The solutions were thermostated to 25°C prior to mixing together. The molar ratios, $X_{IV}=[Na_2O/Al_2O_3]_{bIV}$, $Z_I=[H_2O/Al_2O_3]_{bI}$, $Z_{II}=[H_2O/Al_2O_3]_{bII}$, $Z_{III}=[H_2O/Al_2O_3]_{bIII}$, and $Z_{IV}=[H_2O/Al_2O_3]_{bIV}$, are listed in Table 1 as a functions of the concentrations $[Al_2O_3]_{bI}$, $[Al_2O_3]_{bII}$, $[Al_2O_3]_{bIII}$, and $[Al_2O_3]_{bIV}$, of Al_2O_3 in the systems I, II, III and IV.

Each of the prepared hydrogel was divided in two portions: one portion was put into plastic cuvettes of 50 ml and the other portion was put into PTFE vessels of 50 ml. Both the cuvettes and the PTFE vessels with hydrogels were sealed and kept in a water bath thermostated at 25°C for 48 h.

The hydrogels 'aged' in the cuvettes were centrifuged to separate the solid from the liquid phase. After removal of the supernatant, the solid phase was redispersed in distilled water and centrifuged repeatedly. The procedure was repeated until the pH value of the liquid phase above the sediment was 9. The wet washed solids were dried overnight at 105°C and cooled in a desiccator over silicagel. The dry solids were pulverized in an agate mortar. The pulverized solid samples were kept in a desiccator with saturated NaCl solution for 96 h. Such prepared solids were used for powder X-ray diffractometry and differential thermal gravimetry. A part of each sample was calcined at 800°C for 2 h. After cooling to ambient temperature (in a desiccator over dry silicagel), a

Table 1
Values of $X_N=[Na_2O/Al_2O_3]_{bN}$ and $Z_N=[H_2O/Al_2O_3]_{bN}$ presented as functions of the concentrations $[Al_2O_3]_{bN}$ of Al_2O_3 in batches (batch concentrations of aluminosilicate) of systems (hydrogels) I, II, III and IV (=*N*)

System-batch	$[Al_2O_3]_{bN}$/(mol kg^{-1})	$X_{bN}=[Na_2O/Al_2O_3]_{bN}$	$Z_{bN}=[H_2O/Al_2O_3]_{bN}$
I-1	0.0249	3.00	2206.60
I-2	0.0734	3.00	734.21
I-3	0.1193	3.00	443.00
I-4	0.1640	3.00	316.08
II-1	0.02623	4.15	2086.47
II-2	0.05008	4.15	1077.79
II-3	0.07230	4.15	736.86
II-4	0.09358	4.15	561.12
III-1	0.01234	9.06	4438.33
III-2	0.02433	9.06	2219.68
III-3	0.03598	9.06	1480.33
III-4	0.04735	9.06	1109.96
IV-1	0.0242	21.00	2211.00
IV-2	0.0721	7.00	734.52
IV-3	0.1181	4.20	443.60
IV-4	0.1640	3.00	316.08

given amount of each of the calcined samples was dissolved in 1:1 HCl solution. The obtained solutions were diluted with distilled water to the concentration ranges available for measuring the concentrations of sodium, aluminium and silicon by atomic absorption spectroscopy.

The PTFE vessels with the 'aged' hydrogels were sealed in stainless-steel reaction vessels, put into preheated oven, and heated under static conditions at 80°C until amorphous aluminosilicate was completely transformed to the crystalline phase(s). Thereafter, the reactors were cooled with cold water and the crystalline products were centrifuged to separate from the liquid phase, washed with cold distilled water, and dried overnight at 105°C. The dry crystalline solids were used for powder X-ray diffractometry, scanning-electron microscopy, and determination of particle-size distribution.

Thermogravimetric (TG) and differential thermogravimetric (DTG) analyses of the amorphous solids were performed using a TA 4000 System (Mettler–Toledo) apparatus. The heating rate was 10 K min^{-1} in nitrogen atmosphere.

The X-ray spectra of all samples (washed precipitated solids and the solid phases obtained by the hydrothermal treatment of hydrogels) were taken by a Philips PW 1820 Vertical goniometer mounted on a Philips PW 1300 X-ray generator (Cu K_α radiation) in the corresponding region of Braggs's angles. The weigh fractions of crystalline phases in the powdered samples were calculated by the mixing method [18], using the integral value of the broad amorphous peak and the corresponding sharp peaks of crystalline phase(s).

Scanning-electron micrographs of the crystalline end products obtained by the hydrothermal treatment of hydrogels were taken by a SEM 515 (Philips) scanning-electron microscope.

Particle-size distribution curves of the crystalline end products were determined by a Disc Centrifuge with a photosedimentometer Mark-III (Joyce–Loebl). The mean hydrodynamic particle diameter D and the specific number of particles (particles/g) N_S were calculated from the corresponding particle size distribution curves as

$$D = \frac{\sum \phi_i D_i}{\sum \phi_i} \quad (1)$$

$$N_S = \frac{\sum \phi_i}{\rho \sum \phi_i (D_i)^3} \quad (2)$$

where ϕ_i is the number frequency of the particles

having the hydrodynamic diameter between D and ΔD, $D_i = D + \Delta D/2$ and ρ is the density of the solid phase. The corresponding values of $\sum \phi_i$, $\sum \phi_i D_i$ and $\sum \phi_i (D_i)^3$ were calculated from the particle size distribution curves using the procedures described earlier [19,20].The concentrations of sodium, aluminum, and silicon in solutions were measured by a Perkin–Elmer 3030B atomic absorption spectrometer.

The chemical composition of the solids were calculated from the measured concentrations of Na, Al, and Si in the solutions obtained by dissolution of known quantities of the calcined solid samples in a known volume of the acidified water.

3. Results and Discussion

Powder X-ray diffraction analysis has revealed that, all the solid aluminosilicates separated from systems (hydrogels) I–IV are X-ray amorphous. The results of the chemical analysis of the solids are presented in Table 2. They show that the molar ratio $[SiO_2/Al_2O_3]_S$ in the precipitated solids increases with increasing molar ratio $[SiO_2/Al_2O_3]_{bN}$ of the system (hydrogel). However, the values of $[SiO_2/Al_2O_3]_S$ in the solid phases precipitated at constant molar ratio $[SiO_2/Al_2O_3]_{bN}$ do not depend on the batch molar concentration of aluminosilicate $[Al_2O_3]_{bN}$. The values of the molar ratio $[Na_2O/Al_2O_3]_S > 1$, determined by the chemical analysis of the amorphous solids are somewhat higher than the values, $[Na_2O/Al_2O_3]_S \approx 1$, determined by chemical analysis of supernatants (see Tables 6–8 in [17]). The excess of Na_2O in the solid samples follows from the residual (unwashed) Na_2O [17]. The data presented in the last column of Table 2 show that the content of water in the precipitated solids is not considerably influenced by the chemical composition of the system (hydrogel). The slight simultaneous decrease of the molar ratio $[Na_2O/Al_2O_3]_S$ (see the third column in Table 2) and water content (see the last column in Table 2) with increasing batch concentration $[Al_2O_3]_{bN}$, indicates that part of water molecules arises from the hydration shell of Na^+ ions from residual (unwashed) NaOH in the solid samples [9,17].

Figs. 1–3 shows, the DTG curves of the solid phases (S*N*-1–S*N*-4) precipitated in batches 1 (A), 2 (B), 3 (C), and 4 (D) of systems I (Fig. 1), II (Fig. 2) and III (Fig. 3). The sharp, low-temperature minima (peaks-1) at ca. 60°C in the DTG curves of the solids SI-1 (Fig. 1A), SII-1 (Fig. 2A) and SIII-1 (Fig. 3A) precipitated at the lowest batch concentration of systems I, II and, III correspond to the removal (desorption) of loosely held moisture. The moisture arises mostly

Table 2
Molar ratios $[Na_2O/Al_2O_3]_S$, $[SiO_2/Al_2O_3]_S$ and content of water, $(H_2O)_S$, in the solid samples precipitated from the different batches (1, 2, 3 and 4) of systems (hydrogels) I, II, III and IV. $[Al_2O_3]_{bN}$ is the total amount of Al_2O_3 in the batches of systems I, II and III (=*N*)

Solid	$[Al_2O_3]_{bN}$/(mol kg^{-1})	$[Na_2O/Al_2O_3]_S$	$[SiO_2/Al_2O_3]_S$	$(H_2O)_S$/(wt.%)
SI-1	0.0249	1.416	2.622	26.77
SI-2	0.0734	1.287	2.643	25.33
SI-3	0.1193	1.176	2.660	23.85
SI-4	0.1640	1.096	2.636	21.32
SII-1	0.0262	1.276	2.932	26.75
SII-2	0.0501	1.203	2.924	25.65
SII-3	0.0723	1.103	2.990	23.41
SII-4	0.0936	1.076	2.918	22.08
SIII-1	0.0123	1.342	4.036	25.50
SIII-2	0.0243	1.334	3.973	23.53
SIII-3	0.0360	1.235	4.002	22.11
SIII-4	0.0474	1.268	4.054	22.73
SIV-1	0.0242	1.367	2.628	25.44
SIV-2	0.0721	1.353	2.614	25.14
SVI-3	0.1181	1.145	2.654	22.96
SVI-4=SI-4	0.1640	1.096	2.636	21.32

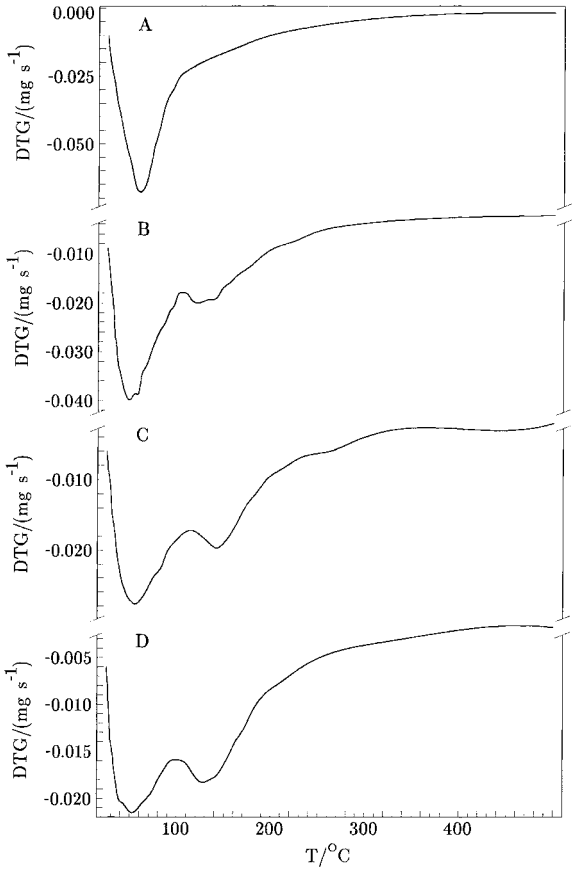

Fig. 1. DTG curves of solids SI-1 (A), SI-2 (B), SI-3 (C) and SI-4 (D) precipitated from batches 1, 2, 3 and 4 of system I.

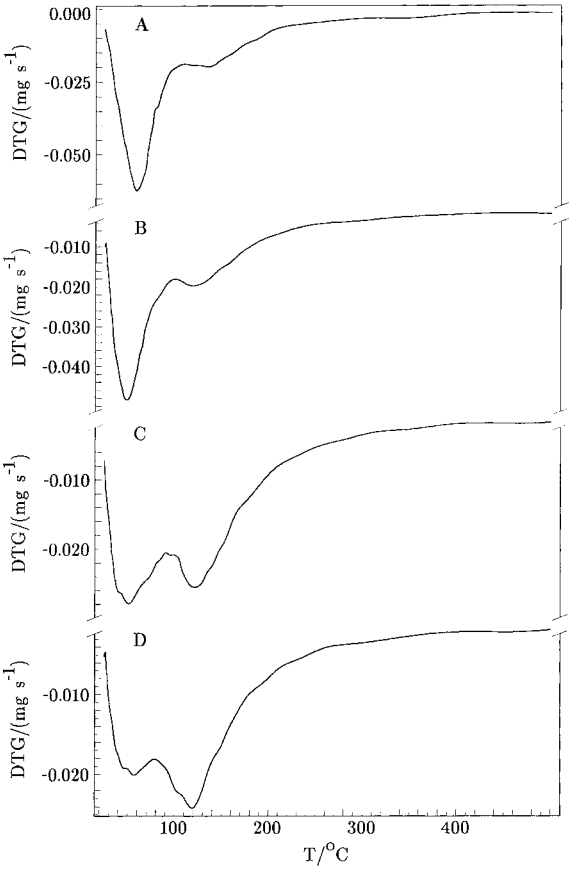

Fig. 2. DTG curves of solids SII-1 (A), SII-2 (B), SII-3 (C) and SII-4 (D) precipitated from batches 1, 2, 3 and 4 of system II.

from the water absorbed at outer and inner surfaces of the gels, and/or from dehydration of Na^+ ions from residual (unwashed) NaOH in the solid samples [9,17]. On the other hand, the appearance of the higher-temperature minima (peaks-2) in the DTG curves of the solids precipitated at increased batch concentration $[Al_2O_3]_{bN}$ is caused by the formation of ordered structural subunits, or even more complex structures (e.g. particles of quasicrystalline zeolite phase) [9–12,14–16,21] inside the matrix of the solid aluminosilicate during its formation in more concentrated sodium–aluminosilicate systems. The position of peak-1 varies between ca. 50°C and 60°C, while the position of the peak-2 varies between ca. 120°C and 150°C (see Table 3). The peak positions do not depend, in an ordered way, either on the batch molar ratio $[SiO_2/Al_2O_3]_{bN}$ (system), or on the batch molar

Table 3
Temperatures of peaks (minimums) in the DTG curves of solids S*N*-1, S*N*-2, S*N*-3, and S*N*-4, precipitated in different batches (1, 2, 3, and 4) of systems I, II and III (=*N*)

Solid	Peak-1/(°C)	Peak-2/(°C)
SI-1	58.5	—
SI-2	48.5	123.2
SI-3	54.7	141.8
SI-4	51.8	129.0
SII-1	58.5	ca. 140*
SII-2	48.5	120.5
SII-3	52.9	122.6
SII-4	55.3	119.3
SIII-1	60.3	ca. 165*
SIII-2	60.3	132.0
SIII-3	54.2	139.3
SIII-4	50.3	147.2

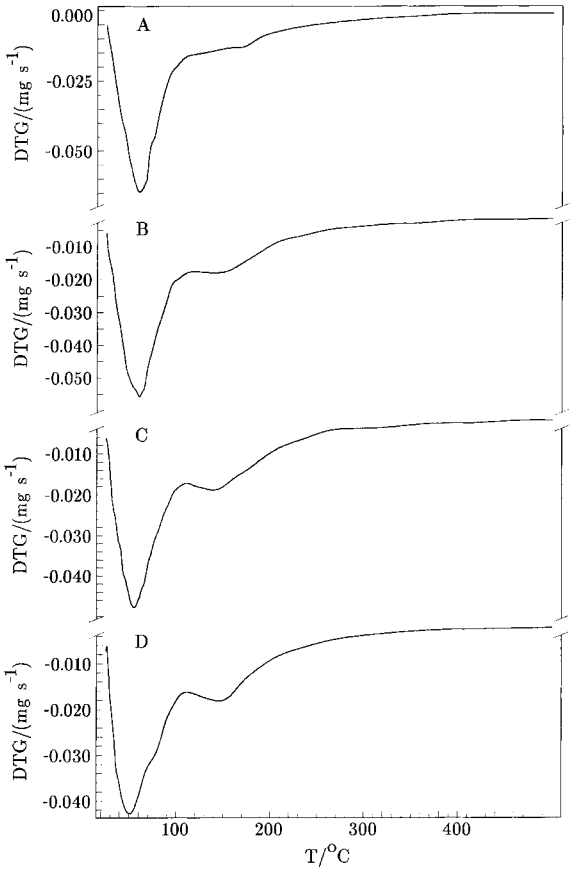

Fig. 3. DTG curves of solids SIII-1 (A), SIII-2 (B), SIII-3 (C) and SIII-4 (D) precipitated from batches 1, 2, 3 and 4 of system III.

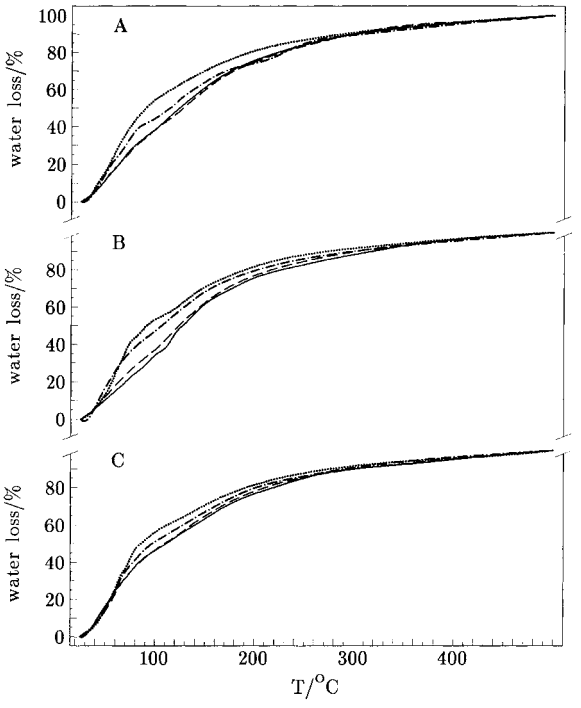

Fig. 4. Percentage of total water, desorbed from solids SI-1, SII-1, SIII-1 (dotted curves), SI-2, SII-2, SIII-2 (dotted-dashed curves), SI-3, SII-3, SIII-3 (dashed curves) and SI-4, SII-4, SIII-4 (solid curves) precipitated from batches 1, 2, 3, and 4 systems I (A), II (B) and III (C), during the controlled heating at a rate of 10 K/min.

concentration $[Al_2O_3]_{bN}$ of a given system. Based on the earlier results of a thermal analysis of the aluminosilicate gels prepared in the presence of 'structure-forming' Li^+ and Na^+ ions as well as 'structure-breaking' K^+ ions [9], one can postulate that the decrease in relative intensity of peak-1 and the simultaneous increase in intensity of peak-2 in the DTG curves of amorphous aluminosilicates is a consequence of the increase in concentration of the quasicrystalline phase in their matrices. [10]. Fig. 4 shows that the rate of water desorption from the gels decreases with increasing batch concentration $[Al_2O_3]_{bN}$, and thus with increasing concentration of structured subunits (quasicrystalline zeolite phase) in the gel matrix. This may be readily explained by the fact that, the energy needed for release of water molecules desorbed from the Na^+ ions positioned in the structured subunits having the channel/void system similar to that of zeolites [22] is higher than the energy needed for release of water molecules desorbed from the Na^+ ions positioned in the amorphous matrix [9]. The consequence is that the desorption of water from the structured subunits occurs at higher temperatures (peaks-2 in the DTG curves shown in Figs. 1–3) than the desorption moisture (peaks-1 in the DTG curves shown in Figs. 1–3).

Pursuing the concept of the formation of structurally ordered subunits inside the amorphous aluminosilicate phase [13] and their role in the nucleation of zeolites [9,10,12–16], one can assume that an increase in concentration of the quasicrystalline phase (potential nuclei) in the aluminosilicate matrix would result in an increasing specific number of zeolite(s) crystals in the final product of the hydrothermal treatment of hydrogels. To prove or disapprove such an assumption, some of selected batches (1, 2, 3, and 4 of system

Table 4
Products obtained by hydrothermal treatment (heating at 80°C for appropriate time) of the selected batches (1, 2, 3 and 4) of systems (hydrogels) I, II, and III

System-batch	Time of heating/h	Product(s)
I-1	720	Amorphous
I-2	480	Zeolite A (100%)
I-3	120	Zeolite A (100%)
I-4	48	Zeolite A (100%)
II-1, II-2, II-3	720	Amorphous
II-4	192	Faujasite (83%) + Zeolite P (17%)
III-1, III-2,III-3	720	Amorphous
III-4	216	Faujasite (67%) + Zeolite P (33%)

I, and 4 of systems II and III) were heated until the solid part of hydrogel (X-ray amorphous aluminosilicate) was completely transformed to the crystalline zeolite phase(s). Table 4 shows that heating of hydrogels I-2, I-3 and I-4 resulted in crystallization of pure zeolite A (see also the scanning-electron micrographs in Fig. 5), and that the time needed for complete transformation increases considerably with decreasing batch molar ratio $[Al_2O_3]_{bI}$. The heating of hydrogel II-4 for 192 h and hydrogel III-4 for 216 h resulted in crystallization of mixtures of faujasite and zeolite P (see Table 4 and the scanning-electron micrographs in Fig. 6). Hydrogels I-1, II-1, II-2, II-3, III-1, III-2 and, III-3 remained amorphous, even after heating at 80°C for 720 h. Since, the alkalinity of batches in a given system decreases proportionally with decreasing batch concentration $[Al_2O_3]_{bN}$ (see Table 5 and [17]), the increase in time of crystallization with decreasing batch concentration was expected. On the other hand, Fig. 5, Fig. 7 and, Table 5 show that the size of zeolite A crystals decreases, and their specific number (number of crystals per gram of product) considerably increases with increasing batch concentration $[Al_2O_3]_{bI}$. These results lead to the conclusion that the concentration of structurally ordered subunits, and hence the specific number of particles of the quasi-crystalline phase increases with increasing batch concentration $[Al_2O_3]_{bI}$. At the same time, these results reveal the postulation that an increase in intensity of peak-2 and a simultaneous decrease in intensity of

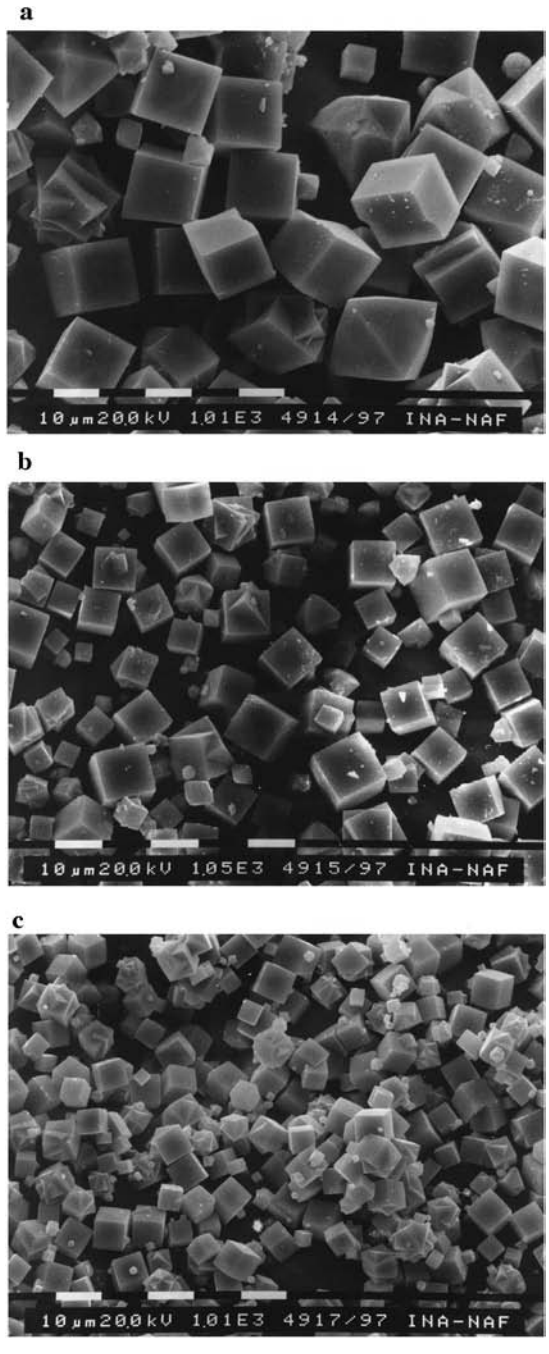

Fig. 5. Scanning-electron micrographs of the crystalline end products (zeolite A microcrystals) obtained by the hydrothermal treatment (heating at 80°C for appropriate time) of batches 2 (A), 3 (B) and, 4 (C) of system (hydrogel) I.

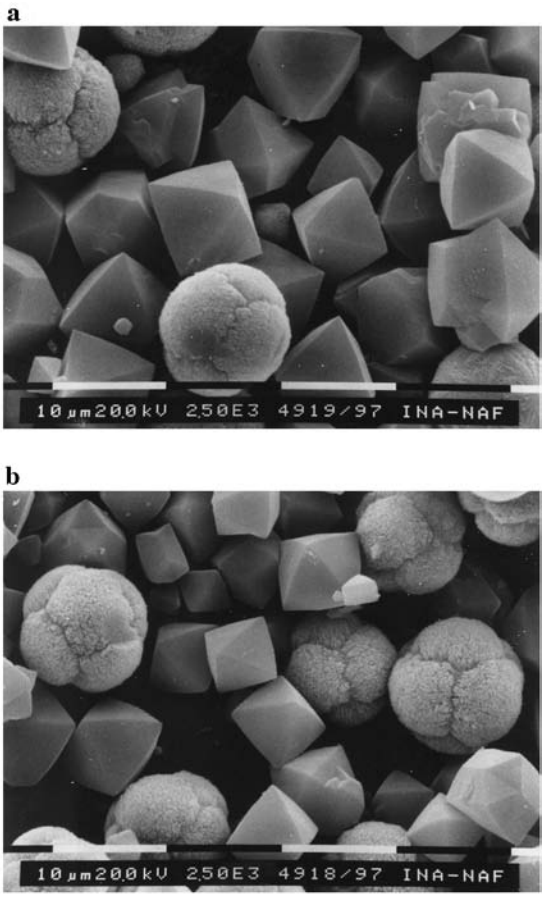

Fig. 6. Scanning-electron micrographs of the crystalline end products (mixture of synthetic faujasite and zeolite P) obtained by the hydrothermal treatment (heating at 80°C for appropriate time) of batches 4 of systems (hydrogels) II (A) and III (B).

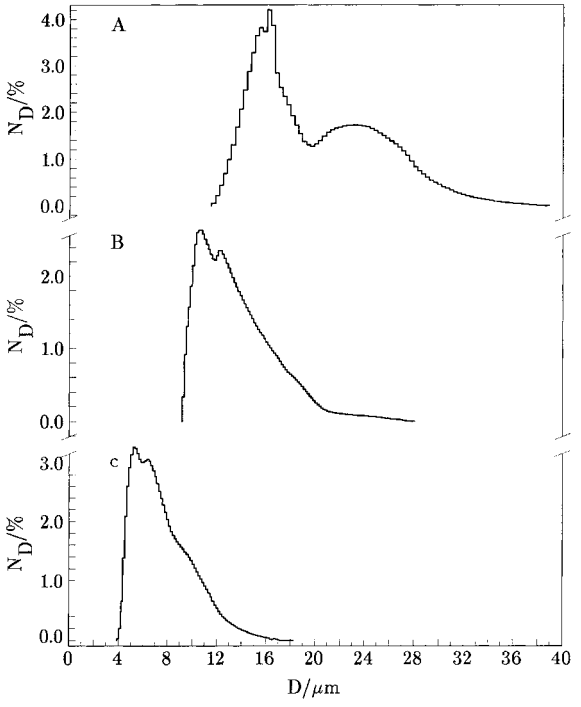

Fig. 7. Particle-size distribution curves of the crystalline end products (zeolite A microcrystals) obtained by the hydrothermal treatment (heating at 80°C for appropriate time) of batches 2 (A), 3 (B), and 4 (C) of system (hydrogel) I. N_D is a number percent of particles with size D.

peak-1 in the DTG curves of the gels is caused by the increase in concentration of the quasicrystalline phase in the gel matrix. However, knowing that alkalinity during the gel preparation has a considerable influence

Table 5
Average size D and specific number of crystals N_S of the crystalline end products (zeolite A) obtained by the hydrothermal treatment (heating at 80°C for appropriate time) of the selected batches (hydrogels), characterized by the batch concentrations $[Al_2O_3]_{bN}$ and $[Na_2O]_{bN}$ of systems I and IV

System-batch	$[Al_2O_3]_{bN}$/(mol kg^{-1})	$[Na_2O]_{bN}$/(mol kg^{-1})	D/µm	N_S/g^{-1}
I-2	0.0734	0.2202	20.12	9.73×10^{7}
I-3	0.1193	0.3579	13.70	3.19×10^{8}
I-4	0.1640	0.4920	7.67	1.61×10^{9}
IV-1	0.0242	0.5082	6.30	3.15×10^{9}
IV-2	0.0721	0.5047	6.64	3.06×10^{9}
IV-3	0.1181	0.4995	8.65	1.08×10^{9}
VI-4=I-4	0.1640	0.4930	7.67	1.61×10^{9}

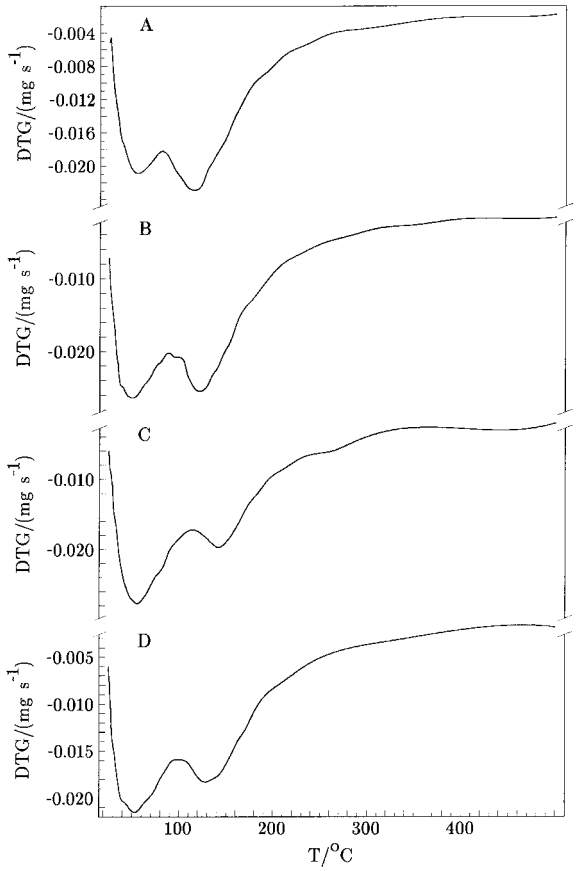

Fig. 8. DTG curves of solids SVI-1 (A), SVI-2 (B), SVI-3 (C), and SVI-4 (D) precipitated from batches 1, 2, 3 and 4 of system (hydrogel) VI.

on the kinetics of nucleation of zeolites, [23] one cannot conclude from these results which of the factors, the concentration of aluminosilicate in the batch or its alkalinity determines the concentration of nuclei in the precipitated amorphous aluminosilicate solid. To clarify this dilemma, the bathes of system I were modified by addition of appropriate amounts of NaOH to aluminate solutions, so that all hydrogels of system I had the same content of Na_2O same as hydrogel I-4 (see Tables 1 and 5). The modified system was designated as system IV. Fig. 8 shows that the addition of NaOH to the batches of system I causes the appearance of a higher-temperature minimum (peak-2) in the DTG curve of solid SIV-1 (see Fig. 8(a)) as well as a decrease in intensity of peak-1 and a simultaneous increase in intensity of peak-2 in the DTG curves of solids SIV-2 and, SIV-3, relative to solids SI-2 and SI-3 (compare Figs. 1 and 8). At the same time, the rate of water desorption is almost the same for all the solids precipitated in system IV and identical to the rate of water desorption from solid SI-4=SIV-4 (see Fig. 9). This leads to an assumption that an increase in batch alkalinity favors the formation of structurally ordered subunits (quasicrystalline zeolite phase) in the aluminosilicate matrix. The results of the hydrothermal treatment of hydrogels IV-1, IV-2, IV-3, IV-4=I-4 confirm such an assumption. The solid phases of all treated batches were transformed to pure zeolite A in less than 48 h (see Table 4). Scanning-electron micrographs (see Fig. 10), particle-size dis-

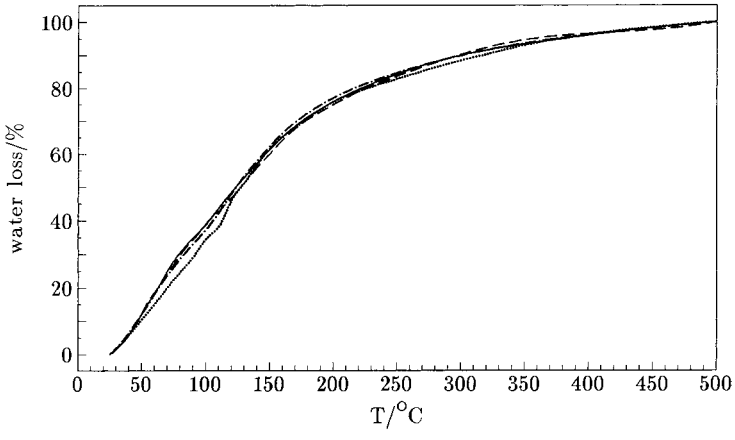

Fig. 9. Percentage of total water, desorbed from solids SVI-1 (dotted curve), SVI-2 (dotted-dashed curve), SVI-3 (dashed curve) and SVI-4 (solid curves) precipitated from bathes 1, 2, 3, and 4 of system VI, during controlled heating at a rate of 10 K/min.

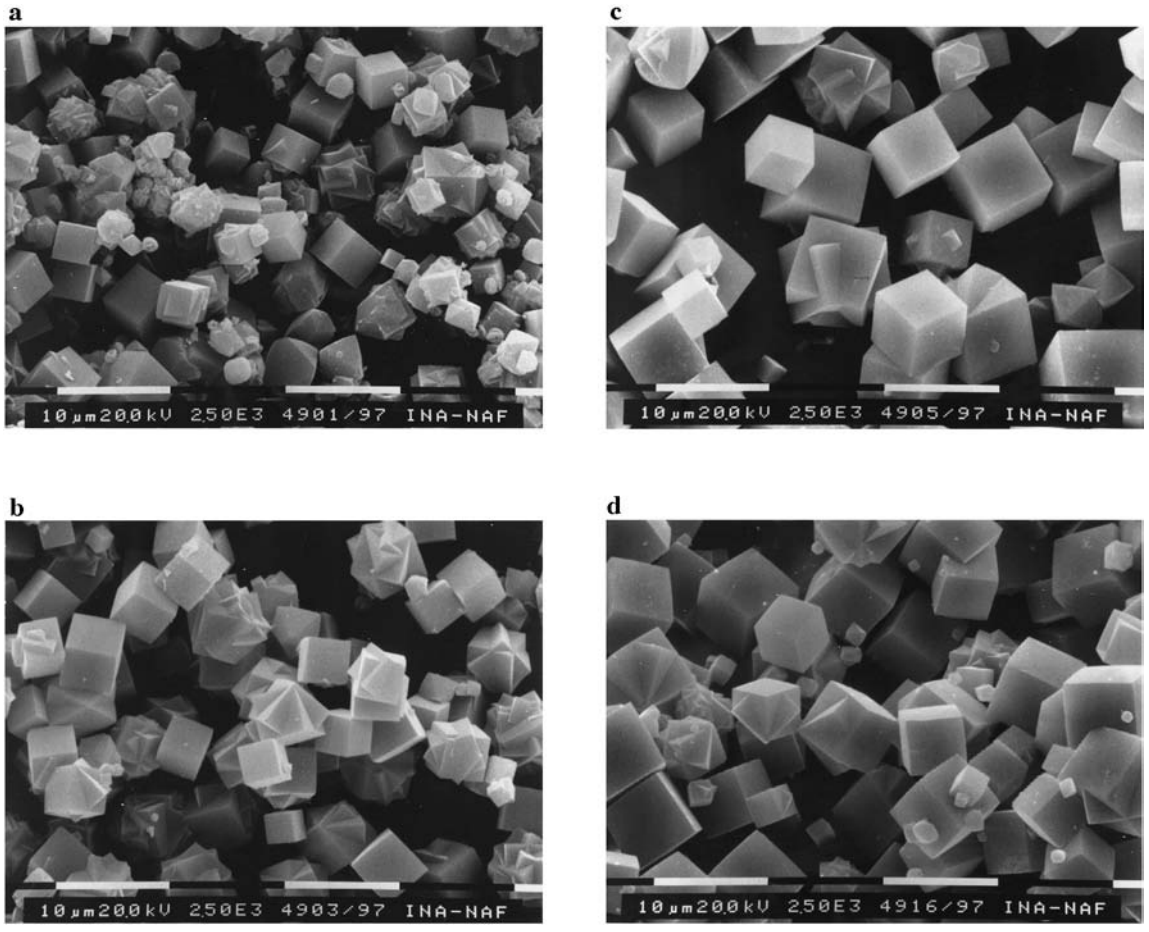

Fig. 10. Scanning-electron micrographs of the crystalline end products (zeolite A microcrystals) obtained by the hydrothermal treatment (heating at 80°C for appropriate time) of batches 1 (A), 2 (B), 3 (C), and 4 (D) of system (hydrogel) IV.

tribution curves (see Fig. 11), average size D of crystals (see Table 5), and the specific number N_S of crystals (see Table 5) of the crystalline end products show that, the particulate properties of zeolite A formed by the hydrothermal treatment of hydrogels IV-1, VI-2 and VI-3 are comparable with the particulate properties of zeolite A formed by the hydrothermal treatment of hydrogel I-4=IV-4. This indicates that the equalization of alkalinity in different batches of system I (system I $\Rightarrow$ system IV) causes the equalization in concentration of structurally ordered subunits (quasicrystalline zeolite phase) in the precipitated amorphous aluminosilicates (gels). Knowing the stabilization role of the 'structure-forming' Na^+ ions in the formation of the subunits which are precursors or nucleation species in zeolite crystallization [24], the influence of alkalinity on the formation of the structurally ordered phase in the gel matrix may be explained as follows: the mechanism of condensation (called 'olation' [25]) requires the presence of negatively charged OH groups for the nucleophilic addition onto a positively charged hydrated metal cation (Na^+). Increasing pH increases the number of negatively charged OH groups in the coordination spheres of Si and Al [25], and thus enhances the reaction of Na^+ ions with aluminate, silicate and/or aluminosilicate species, the formation of structurally ordered phase and its stabilization in the matrix of the precipitated aluminosilicate. However, although alkalinity is a governing factor that controls the structural properties

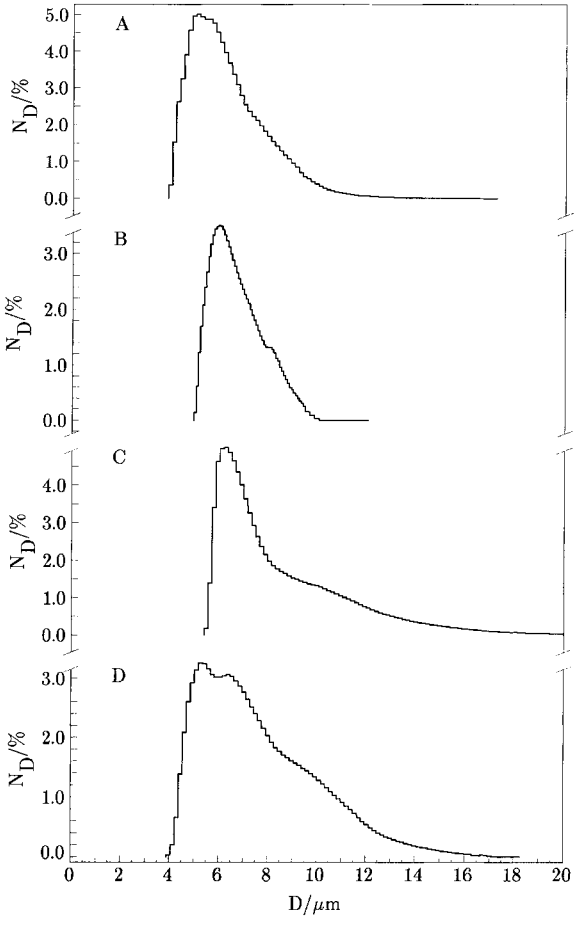

Fig. 11. Particle-size distribution curves of the crystalline end products (zeolite A microcrystals) obtained by the hydrothermal treatment (heating at 80°C for appropriate time) of batches 1 (A), 2 (B), 3 (C), and 4 (D) of system IV. N_D is a number percent of particles with size D.

of the precipitated X-ray amorphous solids, the differences in the particulate properties of the crystalline end products obtained by the hydrothermal treatment of the batches of system IV (see Table 5, and Figs. 9 and 10) indicate that the influence of concentration of the aluminosilicate part of system must not be neglected. The relative influence of the batch concentration $[Al_2O_3]_{bN}$, the alkalinity of the batches and other relevant factors on the specific number of particles of the quasicrystalline phase, their distribution in the aluminosilicate matrix of the precipitated amorphous aluminosilicates, and the influence of the structural properties on the results of the hydrothermal treatment of X-ray amorphous aluminosilicates will be the subject of our further study.

4. Conclusions

Analysis of the results obtained during the thermal (differential thermal gravimetry, DTG) and hydrothermal (heating at 80°C for appropriate time) treatments of X-ray amorphous aluminosilicates prepared at different batch concentrations $[Al_2O_3]_{bN}$ and different batch molar ratios $[SiO_2/Al_2O_3]_{bN}$, have shown the following:

- The sharp, low-temperature minima (peaks-1) at ca. 60°C in the DTG curves of the solids precipitated at the lowest batch concentrations correspond to the removal (desorption) of loosely held moisture. The appearance of the higher-temperature minima (peaks-2) in the DTG curves of the solids precipitated at increased batch concentration $[Al_2O_3]_{bN}$ is caused by the formation of the quasicrystalline zeolite phase inside the matrix of the solid aluminosilicate during its formation in more concentrated sodium–aluminosilicate systems.
- The concentration of the quasicrystalline zeolite phase in the aluminosilicate matrix increases with increasing batch concentration $[Al_2O_3]_{bN}$, as revealed by the results of the hydrothermal treatment of hydrogels, e.g. the specific number of zeolite A crystals (number of crystals per gram of crystallized zeolite A) in the crystalline end products of the hydrothermal treatment increases and their size decreases with increasing batch concentration $[Al_2O_3]_{bN}$. The analysis of the results of the thermal and hydrothermal treatments of hydrogels prepared at different batch concentrations $[Al_2O_3]_{bN}$, and different batch alkalinities have shown that the increase in concentration of the quasicrystalline phase is caused rather by the increase in batch alkalinity than by the increase in concentration of the aluminosilicate part of the system. This has been explained by the fact that the nucleophilic addition of aluminate, silicate, and aluminosilicate species onto Na^+ ions requires the presence of negatively charged OH groups, the concentration of which in the coordination spheres of Al and Si increases with increasing alkalinity of the system.

Acknowledgements

This work was supported by the Ministry of Science and Technology of the Republic of Croatia and by the National Science Foundation (NSF) through mediation of the US–Croatian Joint Board of Scientific and Technological Cooperation.

References

[1] R.C. Mackenzie, in: R.C. Mackenzie (Ed.), Differential Thermal Analysis, vol.1, Academic Press, London, 1970, 498 pp.
[2] W. Smkatz-Kloss, Differential Thermal Analysis, Application and Results in Mineralogy, Springer, Berlin, 1974, 81 pp.
[3] D.N. Todor, Thermal Analysis of Minerals, Abacus Press, Tunbridge, Wels, Kent, UK, 1976, 208 pp.
[4] H.G. McAdie, in: R.C. Mackenzie (Ed.), Differential Thermal Analysis, vol. 1, Academic Press, London, 1970, 449 pp.
[5] C.V. McDaniel, P.K. Maher, in: J.A. Rabo (Ed.), Zeolite Chemistry and Catalysis ACS Monograph 171, American Chemical Society, Washington, DC, 1976, 258 pp.
[6] E.N. Shylyapkina, J. Therm. Anal. 13 (1978) 553.
[7] H.W. Haynes, Catal. Rev. Sci. Eng. 17 (1978) 283.
[8] Z. Gabelica, J.B. Nagy, E.G. Derouane, J.-P. Gilson, Clay Minerals 19 (1984) 803.
[9] R. Aiello, F. Crea, A. Nastro, B. Subotić, F. Testa, Zeolites 11 (1991) 767.
[10] B. Subotić, A.M. Tonejc, D. Bagović, A. Čižmek, T. Antonić, Stud. Surf. Sci. Catal. 84A (1994) 259.
[11] Y. Tsuruta, T. Satoh, T. Yoshida, O. Okumura, S. Ueda, in: Y. Murakami, A. Iijima, J.W. Ward (Eds.), New Development in Zeolite Science, Kodansha, Tokyo, 1986, 1001 pp.
[12] A. Katović, B. Subotić, I. Šmit, LJ.A. Despotović, M. Ćurić, ACS Symp. Ser. 398 (1989) 124.
[13] S.P. Zhdanov, Adv. Chem. Ser. 101 (1971) 20.
[14] B. Subotić, A. Graovac, Stud. Surf. Sci. Catal. 24 (1985) 199.
[15] B. Subotić, ACS Symp. Ser. 398 (1989) 110.
[16] B. Subotić, T. Antonić, I. Šmit, R. Aiello, F. Crea, A. Nastro, F. Testa, in: M.L. Occelli, H. Kessler (Eds.), Synthesis of Porous Materials: Zeolites, Clays and Nanostructures, Marcel Dekker, New York, 1996, 35 pp.
[17] I. Krznarić, T. Antonić, B. Subotić, Zeolites 19 (1997) 29.
[18] L.S. Zevin, L.L. Zavyalova, Kolichestvenniy Rentgenographicheskiy Prazoviy Analiz, Nedra, Moscow, 1974, 37 pp.
[19] B. Subotić, N. Mašić, I. Šmit, Stud. Surf. Sci. Catal. 24 (1985) 207.
[20] Z.I. Kolar, J.J.M. Binsma, B. Subotić, J. Crystal. Growth 116 (1992) 473.
[21] L.A. Bursill, J.M. Thomas, in: R. Sersale, C. Colella, R. Aiello (Eds.), Fifth International Conference on Zeolites, Recent Progress Report and Discussions, Giannini, Naples, Italy, 1981, 25.
[22] C. Kosanović, B. Subotić, A. Čižmek, Thermochim. Acta 276 (1996) 91.
[23] T. Antonić, B. Subotić, N. Stubičar, Zeolites 18 (1997) 291.
[24] E.M. Flanigen, Adv. Chem. Ser. 121 (1973) 119.
[25] J. Livage, Stud. Surf. Sci. Catal. 85 (1994) 1.